

## SPATIALLY VARIED FLOW AT THE TOE OF A ROCK-FILL SLOPE

B. B. SHARP and J. P. JAMES

Dept. of Civil Engineering,  
University of Melbourne, Victoria

**Synopsis**— Water flowing through a rock-fill slope emerges above the toe and passes over the downstream face with water from the lower sections of the rock mass adding to the discharge. This exit phenomenon is a case of spatially varied flow with increasing discharge and is of interest because flow conditions determine the stability of rock-fill slopes subjected to seepage.

A theoretical and experimental investigation was undertaken and results indicated that a solution could be approached if reasonable assumptions were made with respect to the flow conditions in the adjacent body of the slope. This study also provides the basis for a discussion of the problems associated with an exact description of the flow conditions.

### LIST OF SYMBOLS

$a$	Factor dependent on particle shape and surface roughness
$A$	Area of flow
$\alpha'$	Momentum coefficient
$b$	Width of flume
$d$	Diameter of stone
$D$	Distance measured from datum to surface profile
$D_M$	Distance measured from datum to surface of water in manometer
$e$	Void ratio
$g$	Acceleration due to gravity
$h_e$	Exit depth
$h_t$	Depth of tailwater
$h_0$	Height of seepage zone, $h_e - h_t$
$K$	Pitot tube calibration factor
$n$	Porosity
$N$	Head loss coefficient

$q$	Discharge/unit width
$Q$	Discharge
$q^*$	$dQ/dx$
$S$	Energy gradient
$S_0$	Bed slope = $\sin \theta$
$S_f$	Friction gradient
$T$	Surface width
$\theta$	Slope angle
$v$	Velocity of flow
$V$	Mean filter velocity
$V_v$	Mean void velocity
$x$	Distance measured along surface of slope or channel
$y$	Depth of flow (measured normal to slope surface)
$y_c$	Critical depth of flow
$dy/dx$	Gradient of water surface profile relative to the bed

## 1. INTRODUCTION

The construction of Laughing Jack Marsh Dam by the Hydro-Electric Commission, Tasmania,<sup>(1)</sup> has focused interest on the behaviour of rock-fill slopes subjected to seepage.

The flow of water through a slope produces pressure and drag forces on elements both within the body of the slope and on the seepage face. In the design of an earth slope the procedure usually followed is to test only the stability of the slope against sliding without taking into account the local failure that may occur owing to the emergence of seepage. However, investigation has shown<sup>(2)</sup> that in general, as the discharge through a rock-fill slope is increased, rocks are entrained on the seepage face, followed by surface sliding, so that the lower part of the slope assumes a flatter angle. This mechanism of failure has been termed "unravelling" and occurs when the ratio, height of seepage face to diameter of stones, exceeds a certain critical value depending upon the slope angle and material properties.<sup>(3)</sup>

Although, in practice, it is possible to prevent failure by appropriate engineering techniques; e.g. by the use of anchored S.W.R. mesh; this cannot be done economically unless the designer possesses a knowledge of the magnitude and nature of the hydraulic forces acting on the individual rock particles. Obviously this requires a knowledge of the flow characteristics at the toe of the slope.

The two limiting exit conditions at the slope boundary are defined in Fig. 1. The exit depth, i.e. the depth at which the phreatic line intersects the slope boundary, is an important parameter because it remains practically constant until the tail water level reaches the exit depth.<sup>(4)</sup> Referring to the case  $h_e > h_t$  (Fig. 1), the flow through the rock-fill emerges above the toe and passes over the downstream face with water from the rock mass adding to the discharge. Chow<sup>(4)</sup> defines the phenomenon of spatially varied flow as that flow which

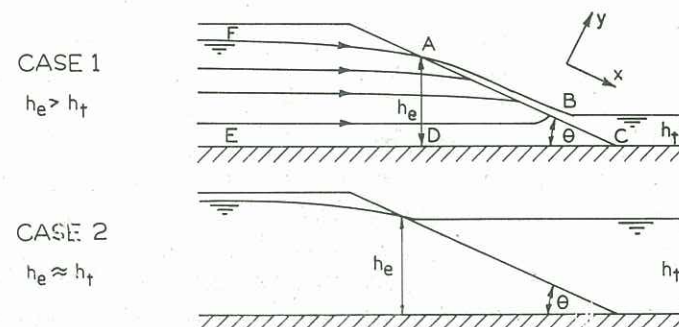


FIG. 1. Exit conditions at a slope boundary.

results when the discharge of a steady flow is non-uniform along the channel:

$$\frac{dQ}{dx} \neq 0$$

Hence in the seepage face of a rock-fill slope the case is one of spatially varied flow with increasing discharge ( $dQ/dx > 0$ ).

## 2. PREVIOUS WORK

### (a) Spatially Varied Flow

Very little has been published about the subject of spatially varied flow and the problem has generally been treated with particular reference to either lateral spillways or surface run-off.

Chow<sup>(4)</sup> developed an equation for spatially varied flow in a channel receiving free discharge from a side spillway. In this development he assumed:



- (i) unidirectional flow,
- (ii) constant and uniform velocity distribution across the channel section,
- (iii) parallel flow,
- (iv) negligible bed slope,
- (v) Manning's formula to evaluate the friction losses due to shear developed along the channel walls,
- (vi) negligible effect of air entrainment,
- (vii) flow depth and velocity increase down the channel and obtained,

$$\frac{dy}{dx} = \frac{S_0 - S_f - 2Qq^*/gA^2}{1 - \frac{Q^2T}{gA^3}} \quad (1)$$

Chow also pointed out that Eq. (1) could be modified to account for a non-uniform velocity distribution in the channel section. However, at the toe of a rock-fill slope, the bed slope and friction gradient are of significant magnitude and cannot be neglected in order to simplify the expression derived by Chow. The further difficulty is that the factor  $q^*$  depends on the slope geometry and rock-fill properties and is of unknown magnitude.

Hauser and Michel<sup>(5)</sup> considered the question of seepage on the downstream slope of a rock-fill dyke and obtained an elaborate expression for the velocity of the surface current:

$$v = 4 \sqrt{g} \cdot \tan^{\frac{1}{5}} \theta \sin^{\frac{3}{10}} \theta d^{\frac{1}{10}} h_0^{\frac{2}{5}} n \quad (2)$$

In this expression,  $n$  is the porosity (vol. voids/total volume), although it is termed the void ratio by both Hauser and Michel and Cohen de Lara<sup>(3)</sup>.

Equation (2) implies that the velocity is constant down the slope. However, Hauser and Michel give no indication as to how the expression was derived, although it appears to be based on an arbitrary roughness equation similar to the Chezy expression. The authors have not been able to derive the same expression.

Connors and Shaw<sup>(6)</sup> studied the flow conditions at the toe of a rock-fill dam in a manner similar to that described below. They obtained a value of  $dQ/dx$  equal to a constant for a slope inclined at 22 degrees to the horizontal and consisting of randomly packed beads. Flow, however, was probably in the transition region between the laminar and turbulent régimes. This result was contrary to previous

research<sup>(7, 8)</sup> but is in agreement with the assumption of a hydrostatic distribution of pressure within the body of the slope and adjacent to the seepage face (see Section 3b). Emery and Sheedy<sup>(7)</sup> obtained an unusual value of  $dQ/dx$ <sup>(8)</sup> because their model was tilted, causing a reduction of  $dQ/dx$  near the toe compatible with long and narrow flow paths to the toe.

#### (b) Pressure Distribution

The flow conditions in the region of the slope adjacent to the downstream face are important. Referring to Fig. 1, it has not been possible to determine mathematical expressions for equipotentials and mean flow paths in the region  $ABCD$  because the flow is turbulent for stones of diameter greater than about 1/2 in.<sup>(1)</sup> Although the two sets are still orthogonal they cannot be made to form curvilinear squares: therefore the flow pattern cannot be found graphically or by techniques involving Laplacian analogues. However, on a model scale the current lines can be made visible by injecting a fluorescein dye<sup>(3)</sup> to display the pattern illustrated in Fig. 1. The flow is approximately tangential to the slope surface at point  $A$  but becomes perpendicular at point  $B$ . However, it remains to be shown whether it is admissible to assume horizontal flow lines beneath the seepage face  $AB$ , corresponding to a hydrostatic distribution of pressure adjacent to the seepage face.

According to Hauser and Michel<sup>(5)</sup>, results of experiments show that for slopes where the downstream slope is inferior to 45 degrees the pressure distribution is practically hydrostatic, although it is more commonly believed that the approximation is sufficiently close only up to a slope angle of about 30 degrees.<sup>(9)</sup>

Cohen de Lara<sup>(3)</sup> used probes to measure the static pressure within a rock-fill wall ( $\theta = 90$  degrees) comprised of 1/4 in. aggregate and noted that, to within 10 per cent, the distribution of pressures along a vertical was hydrostatic except in the immediate vicinity of the downstream end of the wall.

James<sup>(2)</sup> measured the pressure distribution adjacent to the downstream face of a slope comprised of 3/8 in. aggregate heaped at the angle of repose ( $\theta = 40$  degrees). The results were reasonably consistent, with no pressure fluctuations, and proved that, to within 6 per cent, the distribution of pressures along a vertical was hydrostatic. It would be expected that a similar result would hold for a rock-fill slope in which the flow was turbulent ( $d > 1/2$  in.).







Since 
$$H = \frac{\alpha' Q^2}{gby} + \frac{by^2}{2} \cos \theta$$

then 
$$\frac{\partial H}{\partial y} = -\frac{\alpha' Q^2}{gb^2 y^2} + by \cos \theta$$

= 0 at critical depth

Therefore 
$$y_c^3 = \frac{\alpha' Q^2}{gb^2} \cos \theta$$

Assuming  $\alpha' = 1$

Therefore 
$$y_c = \sqrt[3]{\left(\frac{Q^2}{g} \cos \theta\right)} \quad (6)$$

At the critical section

$$y = y_c$$

Substituting  $\alpha' = 1$  and Eq. (6) in Eq. (3)

Therefore 
$$\frac{dy}{dx} = \frac{S_0 - S_f - 2Qq^*/gb^2 y_c^2}{\cos \theta - \cos \theta}$$

It would not be reasonable for this expression to become infinite (which would indicate a profile normal to the bed) and it must therefore be concluded that a solution will be possible only if

$$S_0 - S_f = 2Qq^*/gb^2 y_c^2$$

in which case

$$\frac{dy}{dx} = \frac{2q^*}{Q} \left( \frac{1}{y_c^2} - \frac{1}{y^2} \right) \left( \frac{1}{y_c^3} - \frac{1}{y^3} \right)$$

It now remains to show that this expression tends to a finite limit as  $y$  approaches  $y_c$ , a necessary practical restriction. By the application of l'Hôpital's Rule, it may readily be shown that

$$\lim_{y \rightarrow y_c} \frac{dy}{dx} = \frac{4}{3} \frac{q^*}{Q} y_c$$

which is finite, as required.

If  $\frac{dQ}{dx}$  is linear

$$Q = q^* x$$

Therefore, 
$$S_0 - S_f = \frac{2Q^2}{x} / gb^2 y_c^2 = \frac{2y_c \cos \theta}{x}$$

Therefore, 
$$x^3 = \frac{8y_c^3 \cos^3 \theta}{(S_0 - S_f)^3} = \frac{8q^{*2} x^2 \cos^2 \theta}{gb^2 (S_0 - S_f)^3}$$

and 
$$x = \frac{8q^{*2} \cos^2 \theta}{gb^2 (S_0 - S_f)^3}$$

If friction is ignored the critical section occurs at

$$x = \frac{8 \cos^2 \theta q^{*2}}{gb^2 \sin^3 \theta} \quad (7)$$

Tests at the University of Melbourne<sup>(6)</sup> have shown that it is not permissible to estimate the friction gradient from the Manning or Chezy formula using empirical values of  $n$  and  $C$  respectively. It is apparent that for the case of spatially varied flow at the toe of a rock-fill slope the incoming fluid alters the boundary layer flow conditions. However, research into the problem is not sufficiently advanced to warrant further discussion at this time.

#### 4. EXPERIMENTAL PROGRAMME

A model slope was constructed of nominal  $\frac{3}{4}$  in. diameter crushed basalt aggregate in a rectangular flume 3 ft long  $\times$  1 ft 6 in. high  $\times$  1 ft wide. The front panel of the flume consisted of a Perspex window so that flow phenomena could be observed.

The relevant data for the slope are

$$\theta = 25.2^\circ$$

$$e = 0.73$$

The surface of the slope was stabilized with  $\frac{1}{2}$  in. wire mesh. In this regard the size of the mesh needed to be large enough to prevent disturbance of the flow and yet small enough to hold the aggregate in place.

A foam plastic baffle was used to ensure uniform flow at inlet (Fig. 4). The flow on the slope was made independent of downstream conditions by arranging for free-fall exit discharge at the toe of the slope.

A constant discharge was passed through the slope (Fig. 4). The depth and velocity of the filament of water on the downstream



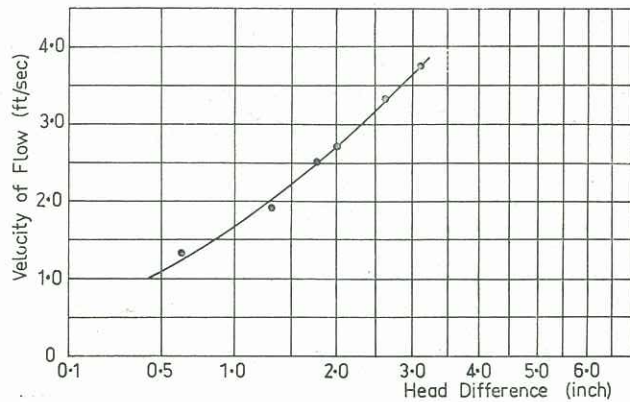


FIG. 3. Calibration curve for pitot tube.

face were measured at 20 sections along the slope, adopting the mean of 5 readings taken across the width of the slope at each section (Fig. 5).

The depth of flow was measured with a scaled pointer and the readings taken to an accuracy of 1/100 in. However, due to irregularities of the slope, this accuracy is rather spurious. The variation across the width of the slope was considerable at some sections, although the nature of the depth profile plotted on Fig. 5 suggests that the mean values were quite reasonable. The pointer reading was multiplied by  $\cos \theta$  to give the depth of flow.

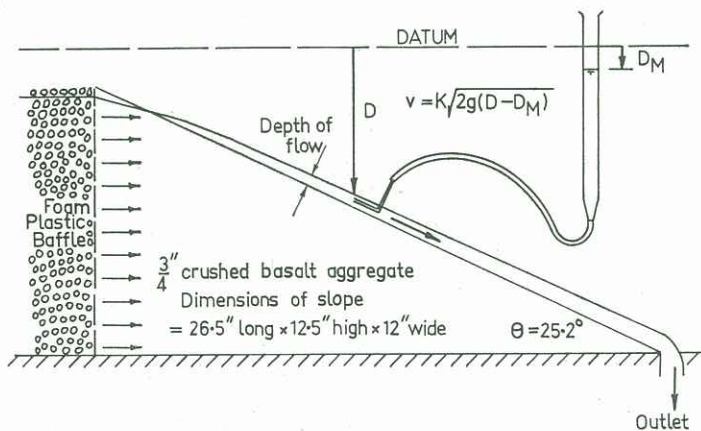


FIG. 4. Method of measuring velocities.

Various methods of measuring small velocities in thin layers of flow were investigated.<sup>(7)</sup> A fine glass pitot tube was adopted as the most satisfactory method of measuring the velocity. The pitot tube was assumed to possess a characteristic:

$$v = K \sqrt{[2g (D - D_m)]} \quad (\text{see Fig. 4})$$

In order to measure the calibration factor, ( $K$ ), flows of average velocities throughout the expected range were established in a long rectangular flume (6 in. wide). Normal depth was assumed at about the mid point of the flume and the same depth was maintained for each flow by altering both slope and discharge. In this manner the velocity contours were expected to have a similar form for all flows

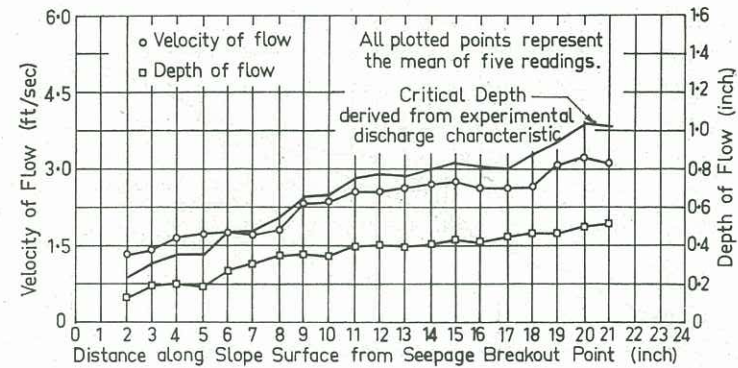


FIG. 5. Velocities and depths down a model slope.

The average velocity head in the flume was determined for each flow by taking pitot tube readings at 8 points below the water surface and in a definite pattern. Comparison with the measured discharges enabled  $K$  to be determined (Fig. 3). Due allowance was made for capillarity in the  $\frac{1}{2}$  in. diameter glass manometer tube throughout the testing programme. The pitot tube was clamped in position prior to each reading and water was added to the manometer so that the equilibrium position was always reached by the water level falling in the manometer.

### 5. PRESENTATION AND DISCUSSION OF RESULTS

The mean values of flow depth and velocity are plotted on Fig. 5. The discharge was obtained from these values and is plotted on Fig. 6.

In the calibration of the pitot tube, a high degree of accuracy was attainable, since the discharge and depth of flow were large.



However, in the experiment on the model, it is unreal to claim a particular degree of accuracy because of the relatively small quantities involved, and the non-uniform conditions of flow produced by the irregular nature of the slope surface. However, the fact that the curves plotted on Fig. 5 have a consistent form indicates that the results are acceptable.

The exact origin of flow was difficult to determine visually but appeared to be located 2 in. upstream of the first section of measurement.

Referring to Eq. (5), Parkin<sup>(10)</sup> gives  $a=1.86$  ft-sec units and  $N=0.54$  for the particular  $\frac{3}{4}$  in. aggregate used in the experiment.

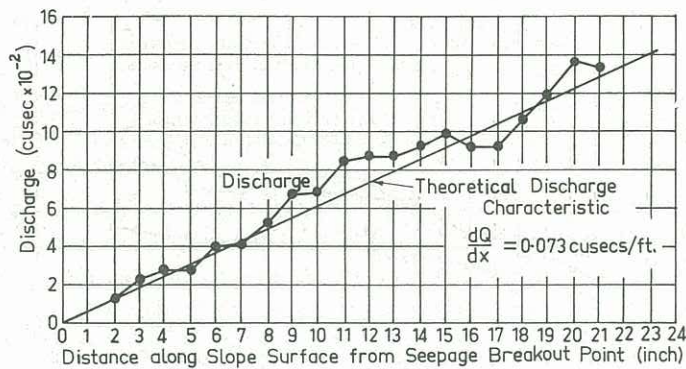


FIG. 6. Comparison of computed and measured discharge rates.

However these values were obtained for a void ratio of 1.0 whereas the material was placed at  $e=0.73$  in the model slope. The results are readily modified for this condition<sup>(10)</sup> to give the theoretical value of  $dQ/dx$ :

$$\begin{aligned} \frac{dQ}{dx} &= \left(\frac{0.73}{1.0}\right)^{0.5} \left(\frac{0.73}{1.73}\right) \left(\frac{\tan 25.2^\circ}{1.86}\right)^{0.54} \sin 25.2^\circ \\ &= 0.854 \times 0.422 \times 0.475 \times 0.426 \\ &= 0.073 \text{ cusecs/ft} \end{aligned}$$

This result is plotted on Fig. 6 and gives a discharge characteristic that is consistent with the experimental results.

It is also observed (Fig. 5) that the velocity and depth of flow increase down the slope. The assumption made in the derivation

of the dynamic equation for spatially varied flow with increasing discharge for a steep slope (Section 3a) is thus substantiated. It is also emphasized that the velocity of the current on the slope is not constant as implied by Hauser and Michel<sup>(5)</sup>.

The critical depth is greater than the flow depth over the full range of measurement (Fig. 5). This means that the critical section is very near the origin of flow and the flow is nearly all rapid. Substitution of the relevant values in Eq. (7) leads to:

$$x=0.17 \text{ in.}$$

Although the effect of friction is to increase this value, the result suggests that  $S_0 > S_f$  for a steep rock-fill slope.

It has already been mentioned (Section 3c), that the nature and magnitude of the friction gradient along the bed is not properly understood. The friction gradient is certainly of significant magnitude and it is unrealistic to simplify the problem by assuming  $S_f=0$ . Hence it has not been possible to plot a theoretical flow profile to enable comparison with the measured values of the depth of flow. However, it is hoped that current research will be able to resolve this problem.

## CONCLUSIONS

The dynamic equation for spatially varied flow at the toe of a rock-fill slope has been derived. In this regard, the modification of Eq. (1) for application to steep slopes was an essential requirement of the investigation. The solution of the equation involves a knowledge of the nature and magnitude of the discharge characteristic  $dQ/dx$ , and the friction gradient  $S_f$ .

An empirical formula, based on the assumption of horizontal flow lines beneath the slope, is proposed which shows good agreement with tests. The linear nature of this relationship, which gives  $dQ/dx$  in terms of the slope geometry and material properties, is emphasized.

The criteria for determination of the critical section were investigated and, for the case  $q^*=const.$ , a simple formula is obtained. The concept of critical depth is identical for spatially varied flow and constant discharge flow, using both energy and momentum principles, provided that partial derivatives are taken in the former case.



Further work is required to determine the effect on the friction factor of the velocity of the incoming fluid, and to determine the applicability of the Manning or Chezy formula to very steep slopes.

#### ACKNOWLEDGEMENTS

The work described in this paper was stimulated by an investigation into the hydraulic characteristics of rock-fill dams sponsored by the Water Research Foundation of Australia Ltd.

A substantial part of the investigation was carried out by final year civil engineering students during the period 1960-1962. In this regard thanks are due to Messrs. J. C. Emery, B. J. Sheedy, G. F. Connors, M. B. Shaw and B. E. Foley.

#### REFERENCES

1. LAWSON, J. D., TROLLOPE, D. H. and PARKIN, A. K., Some hydraulic aspects of unconventional rockfill dams, Paper Presented to Conf. on Hydraulics and Fluid Mechanics, University of W. A. (1962).
2. JAMES, J. P., The stability of a simple rock-fill slope subjected to seepage, M.Eng.Sc. Thesis, University of Melbourne (1962).
3. COHEN DE LARA, G., A study of seepage in rip-rap dams. Application to the case of cut-off coffer dams, Fourth Hydraulic Conf., Paris, Sec. 4, No. 7 (1956).
4. CHOW, VEN TE, *Open Channel Hydraulics*, McGraw-Hill (1959).
5. HAUSER, R. and MICHEL, B., Stability of the downstream slope of rock-fill dykes, Proc. Eighth Congress, International Assoc. for Hydraulic Research, Vol. 4 (1959).
6. CONNORS, G. F. and SHAW, M. B., Spatially varied flow at the toe of a rockfill dam, Research Project, Civil Engineering Dept. University of Melbourne (1961).
7. EMERY, J. C. and SHEEDY, B. J., Spatially varied flow at toe of rockfill dam, Project, Civil Engineering Dept. University of Melbourne (1960).
8. SHARP, B. B., Flow in a rock-fill dam with inbuilt spillway, *Civil Engineering*, 56, No. 665 (1961).
9. LELIAVSKY, S., *Irrigation and Hydraulic Design*, Vol. 1, Chapman and Hall, London (1955).
10. PARKIN, A. K., Rockfill dams with inbuilt spillways. Part 1. Hydraulic characteristics. University of Melbourne. Report to the Water Research Foundation of Aust. Ltd., No. DR 2 (Sept. 1962).
11. LI, W. H., Open channels with non-uniform discharge, *Trans. A.S.C.E.* 120 (1955).

## AN EXACT THEORY OF SIMPLE FINITE SHALLOW WATER OSCILLATIONS ON A ROTATING EARTH

F. K. BALL

C.S.I.R.O. Div. Meteorological Physics,  
Aspendale, Victoria

**Synopsis** — Instead of attempting to find exact solutions for the finite motion of a shallow liquid lying on a surface of given shape, simple forms of solution are assumed and the shape of the underlying surface necessary for such motions to occur is then determined. Two simple types of motion are considered.

(a) Pure displacement, where the liquid is displaced laterally without distortion of the depth profile and the horizontal velocity is a function of time only.

(b) Simple distortion and rotation, where the centre of gravity of the liquid remains stationary and the horizontal velocity is a linear function of the space coordinates.

Both types of motion can only occur on a paraboloidal surface, including a level surface as an important special case.

In this way, exact solutions can be derived not only for finite oscillatory motions in paraboloidal bowls but also for the gravitational collapse of a liquid dome. Furthermore, despite the non-linearity of the basic equations, the displacement motion is independent of other motions and the two types of solution can be combined to give further solutions.

#### LIST OF SYMBOLS

$A, B$	Arbitrary constants
$b$	Initial radius of liquid undergoing pure distension
$E$	Total energy of liquid
$f$	Coriolis parameter of the earth's rotation
$F, G$	Arbitrary functions of $r/k$
$g$	Gravitational acceleration
$H$	Depth of liquid at its midpoint
$h$	Depth of liquid
$J$	Absolute angular momentum of liquid